



HAL
open science

Experimental validation of a fluid dynamics based model of the UF Falcon concentrator in the ultrafine range

Jean-Sébastien Kroll-Rabotin, Florent Bourgeois, Eric Climent

► To cite this version:

Jean-Sébastien Kroll-Rabotin, Florent Bourgeois, Eric Climent. Experimental validation of a fluid dynamics based model of the UF Falcon concentrator in the ultrafine range. *Separation and Purification Technology*, 2012, 92, pp.129-135. 10.1016/j.seppur.2011.10.029 . hal-02086240

HAL Id: hal-02086240

<https://hal.science/hal-02086240>

Submitted on 28 Mar 2024

HAL is a multi-disciplinary open access archive for the deposit and dissemination of scientific research documents, whether they are published or not. The documents may come from teaching and research institutions in France or abroad, or from public or private research centers.

L'archive ouverte pluridisciplinaire **HAL**, est destinée au dépôt et à la diffusion de documents scientifiques de niveau recherche, publiés ou non, émanant des établissements d'enseignement et de recherche français ou étrangers, des laboratoires publics ou privés.



Open Archive Toulouse Archive Ouverte (OATAO)

OATAO is an open access repository that collects the work of Toulouse researchers and makes it freely available over the web where possible.

This is an publisher-deposited version published in: <http://oatao.univ-toulouse.fr/>
Eprints ID: 5071

To link to this article: DOI:10.1016/j.seppur.2011.10.029
<http://dx.doi.org/10.1016/j.seppur.2011.10.029>

To cite this version:

Kroll-Rabotin, Jean-Sébastien and Bourgeois, Florent and Climent, Eric
*Experimental validation of a fluid dynamics based model of the UF Falcon
concentrator in the ultrafine range .* (2012) Separation and Purification
Technology, vol. 92. pp. 129-135. ISSN 1383-5866

Any correspondence concerning this service should be sent to the repository
administrator: staff-oatao@inp-toulouse.fr

Experimental validation of a fluid dynamics based model of the UF Falcon concentrator in the ultrafine range

Jean-Sébastien Kroll-Rabotin^{a,c}, Florent Bourgeois^{a,c,*}, Éric Climent^{b,c}

^a Université de Toulouse, INPT, UPS Laboratoire de Génie Chimique, 4 Allée Emile Monso – BP 44362, 31432 Toulouse Cedex 4, France

^b Université de Toulouse, INPT, UPS, Institut de Mécanique des Fluides, Allée Camille Soula, F-31400 Toulouse, France

^c CNRS, Fédération de recherche FERMAT, Toulouse, France

A B S T R A C T

The process of separating ultrafine particles, say below 80 μm , on the basis of density is a true technical challenge. Indeed, the separation process itself becomes very much size dependent with such fine particles, so that large enough density differentials are necessary for offsetting the strong particle size effect. Our study is concerned with understanding the limitations of the UF Falcon concentrator, an enhanced gravity separator specifically designed for treating slurries with ultrafines. To this end, based on a number of hypotheses, we have already derived and published a theoretical model of the UF Falcon concentrator for treating dilute suspensions. This paper presents the validation and calibration of this model, based on experimental measurements carried out under controlled conditions using a laboratory scale concentrator. By comparing measured and predicted separation results for particles with known size distribution and density, the work validates the key model hypotheses, thereby confirming our understanding of the physics of the separation process. Moreover, by changing operating conditions in a systematic manner, the work is able to calibrate the model so that it can be used to make quantitative prediction of the UF Falcons performance.

Keywords:

Gravity concentration

Modeling

Fine particle beneficiation

1. Introduction

Amongst enhanced gravity separators [1–3], Falcon concentrators [4,5] have found a wide number of applications in industry for separating and concentrating mineral slurries on the basis of particles specific gravity. The enhanced gravity field created by their fast spinning bowl can reach several hundred times the Earths gravitational acceleration. The strong increase in differential settling velocities that results allows such separators to handle significant tonnages of fine and ultrafine particle suspensions [6,7].

The Falcon UF series consists of a fast spinning conical bowl fed at its center. Due to the combined effect of bowl opening angle and centrifugal force, the slurry flows upwards along the bowl wall (see Fig. 1). A slight reduction in diameter at the outlet retains the concentrate inside the bowl while the tailings escape continuously through the top of the separator. In other words, heavy particles are trapped in the retention zone while light particles exit with the process water. Experiments presented hereafter were carried out with an L40 Falcon concentrator fitted with a UF shaped

smooth bowl (4" diameter). It is a semi-batch device in which concentrate retention is achieved by a lip, that is a slight diameter decrease at the outlet. So, the concentrate can only be recovered manually by stopping the process, whereas the tailings stream is rejected continuously during operation.

Our analysis [8–10] of the physics of the separation process inside a UF Falcon concentrator led us to make the following hypotheses:

- Particle settling along the centrifugal gravity is the main separation mechanism.
- Particles that enter the Falcon bowls retention zone cannot be resuspended back into the flowing film.
- The flow field inside the flowing film can be modeled by a Poiseuille's semi-parabolic profile and a solid rotation.
- At the bottom of the bowl, the impeller mixes the suspension homogeneously.
- The action of the fluid on the particles can be described by a Stokes' law whose drag coefficient is inversely proportional to the particulate Reynolds number.

Under these hypotheses, to which simplifying hypotheses about the physics of fluid and particle transport were added [8], we were able to predict the trajectory of particles for dilute suspensions (i.e. solids concentration less than 5 vol.%) inside the film that flows on

* Corresponding author at: Laboratoire de Génie Chimique, 4 Allée Emile Monso – BP 44362, 31432 Toulouse Cedex 4, France. Tel.: +33 5 34 32 36 33.

E-mail addresses: jeansebastien.krollrabotin@ensiacet.fr (J.-S. Kroll-Rabotin), florent.bourgeois@ensiacet.fr (F. Bourgeois), climent@imff.fr (É. Climent).

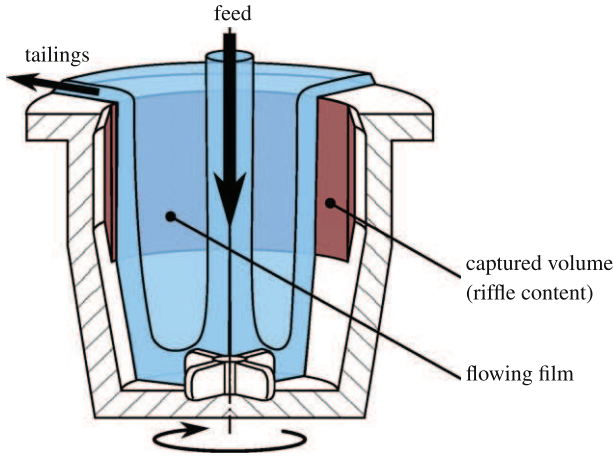


Fig. 1. Falcon smooth bowl schematics.

the surface of the bowl. We derived an analytical expression for the distance (L) a particle travels from the center of the separator. This length depends on particle properties (radius r_p and density ρ_p), fluid properties (density ρ_f and dynamic viscosity μ), operating conditions (feed volumetric flowrate Q and bowl speed ω), bowl geometry (base radius R_0 , opening angle β and bowl length L_{bowl}), the film thickness h , and the elevation Y_0 inside the film thickness at which the particle is injected at the base of the bowl. The reasoning behind this approach is that any particle whose travel length L is less than the length of the bowl L_{bowl} will report to the concentrate. From the analytical expression for L , we derived the following expression for the partition function [9,10]:

$$C_p = \min \left(\frac{4\pi}{9} \lambda Q^{-1} \omega^2 (\rho_p - \rho_f) r_p^2 \mu^{-1} R_0^{2-\alpha} \cos \frac{\beta}{2} L_{\text{bowl}}^{1+\alpha}, 1 \right), \quad (1a)$$

$$\text{where } \alpha = \frac{\ln \left(1 + \frac{L}{R_0} \sin \frac{\beta}{2} \right)}{\ln \frac{L}{R_0}}. \quad (1b)$$

The full details of the derivation that led to Eq. (1a) can be found in [8]. The justification for the calibration constant λ will be given in Section 3.2. Although the above expression applies to dilute suspensions only, Eq. (2) was eventually modified to account for solids concentration. For the reader's sake, we decided to present the final version of the model hereafter:

$$C_p = \min \left(\frac{4\pi}{9} \lambda (1 - 1.6\phi) Q^{-1} \omega^2 (\rho_p - \rho_s) r_p^2 \mu^{-1} R_0^{2-\alpha} \cos \frac{\beta}{2} L_{\text{bowl}}^{1+\alpha}, 1 \right). \quad (2)$$

Compared with the dilute model, the concentrated model requires specification of a solids volume concentration ϕ and a suspension density ρ_s . It was determined that ϕ should be the volume fraction of the feed stream and ρ_s should be the suspension density in the tailings, which implies an iterative scheme for using Eq. (2). The derivation and validation of the concentrated model will be discussed in an upcoming publication. With the present paper, we restrict our discussion to the validation of the dilute model, which in effect validates the model hypotheses of the proposed Falcon model. First, we discuss the testing and validation of the model assumptions, and then the calibration of the model for predictive purposes.

2. Materials and methods

Our experimental set-up consists of a L40 Falcon concentrator that can be operated at controlled bowl speed and feed flow rate.

The test rig (see Fig. 11) includes a Falcon L40 concentrator with a UF bowl, a peristaltic pump (type: PCM Delasco 1.3Z3; motor: NORD SK 71S/4TF), an electronic scale for on-line mass flow measurements, and a number of ancillaries (agitated feed sump, constant head feed tank, by-pass for running in closed circuit, flow rate adjustment valve, pipes and fittings).

The overflow rate is monitored continuously by an electronic scale. Overflow samples are taken at chosen times during an experiment diverting the whole overflow stream to sample containers. With every test run, feed size distribution and solids content are also checked for mass balance.

For the purpose of model validation, we have used well-characterized silica particles. This material permits generation of controlled suspensions with known washability distributions for hypotheses testing and model calibration. Within the framework of this paper, only dilute suspensions (i.e. solids content less than 5 vol.%) are considered.

2.1. Feed to the Falcon separator

The test rig uses a 20-L agitated sump that can hold the whole circuit feed volume. A 5-L agitated tank, which is fed from the sump through a peristaltic pump is placed directly above the Falcon. The water level is kept constant in this tank by an overflow pipe, so that the Falcon is gravity fed with constant pressure head, hence constant flowrate. A gate valve is located below this tank to adjust the flow rate that feeds the Falcon. This set-up ensures that the Falcon feed flow rate remains constant during a test although the total amount of available suspension decreases as a result of particle capture and overflow sample collection.

Prior to feeding the Falcon, the feed valve is closed to bypass the Falcon separator so the system runs in closed circuit, which serves to homogenize the slurry throughout the system. The bypass is opened once steady state is reached. The residence time inside the Falcon is so short (<0.05 s) that it can be assumed that the overflow is established instantaneously (typical experimental run duration is between 1 and 2 min for dilute feed suspensions).

2.2. Suspension samples

Separation efficiency is measured by comparing feed washability with the washabilities of the concentrate and tailings streams. Washability measurement, which requires separation of particles according to both size and density is particularly difficult with ultrafine particles. Standard ways exist however for measuring particle size distribution in the ultrafine range, such as laser diffraction. In our work, we use a Malvern Mastersizer 2000 [11] with single material suspensions, for which particles have the same density and optical properties.

As discussed earlier, we identified differential settling as the governing separation mechanism for the UF Falcon separator. Hence, the relevant particle size required by our model is the Stokes diameter [12]. Since the particles we used are close to spherical in shape, it is fair to assimilate particle size measured by laser diffraction to Stokes size.

The commercial silica we used is more than 98% SiO_2 , so we consider it to follow a single density distribution. The size distribution, measured by Malvern Mastersizer 2000 with the optical properties presented in Table 1, is plotted in Fig. 2. Identical 75 μm

Table 1
Optical properties of used material.

	Refraction index	Absorption index
Silica	1.485	0.0

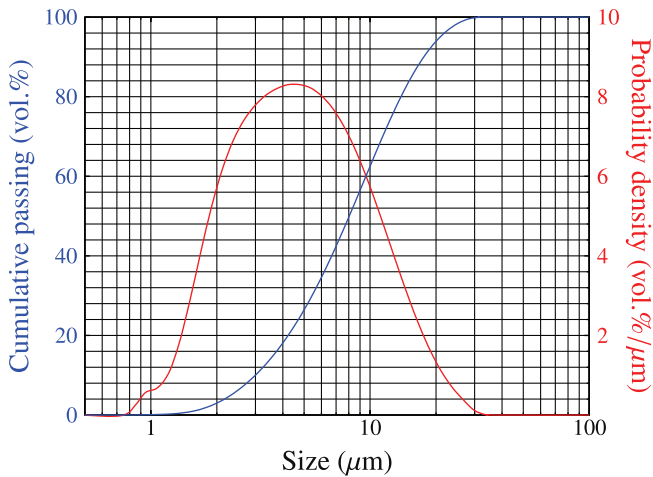


Fig. 2. Size distribution of the silica suspension.

samples were produced for testing by splitting a 5 kg lot using a Retsch PT 100 rotary sample divider. It is noted that measurement of silica size distribution by laser sizing was found to be highly sensitive to the chosen refractive index. To avoid optical artefacts in the measured size distribution, the correct index had to be determined experimentally by minimizing the residuals of the diffraction pattern fitting achieved by laser sizer [11].

2.3. Measurements

With the L40 semi-batch separator, only the feed and tailings streams can be sampled over time without stopping operation. The concentrate stream, which accumulates inside the bowl during a test run, can only be analyzed at the end of an experiment. If separation inside the Falcon happens to change over time, the washability of the final concentrate does not correspond to the separation at any specific time during the experiment, but is instead a measure of the average separation that took place inside the Falcon over the duration of the test.

Sampling two of the three process streams – feed and overflow – is not sufficient for reconciling the data and calculating the experimental partition function. Fortunately, we demonstrated (see Section 3.1) that during a long enough period of time, which corresponds to the time necessary to fill the retention zone, the separation inside the UF Falcon does not change. Hence, the size distribution of the concentrate stream could be measured simply by stopping the test before the retention zone is filled, and by sampling the particles concentrated inside the bowl. Material balance could therefore be done on a size-by-size basis, yielding the solids split and the partition function for any given test run.

3. Results

The experimental results that are presented in the paper address two distinct issues. The first one concerns the validation of our model hypotheses, which reflect our understanding of the physics of the UF Falcon. The second one deals with the validation of the analytical prediction of the model under dilute conditions (cf. Eq. (1a)) the calibration of the model's single constant.

3.1. Validation of the no-resuspension assumption

From the observations made by [7] about the build-up of the concentrate bed inside the Falcon concentrator, we deduced that resuspension of particles from the bed to the flowing film is negli-

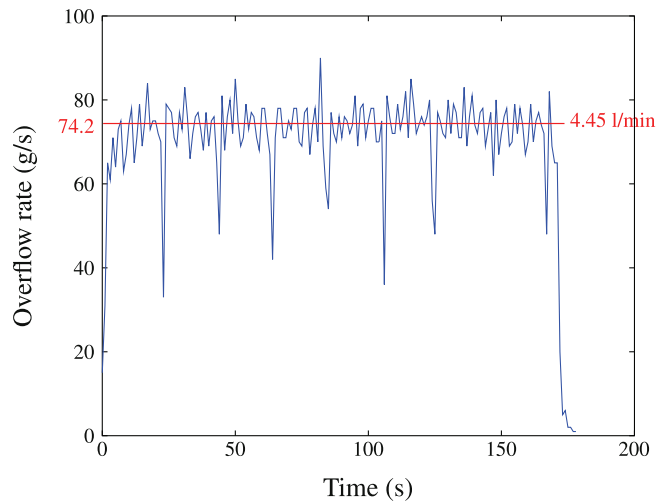


Fig. 3. Overflow rate over time for the riffle saturation experiment (operating at 1460 rpm).

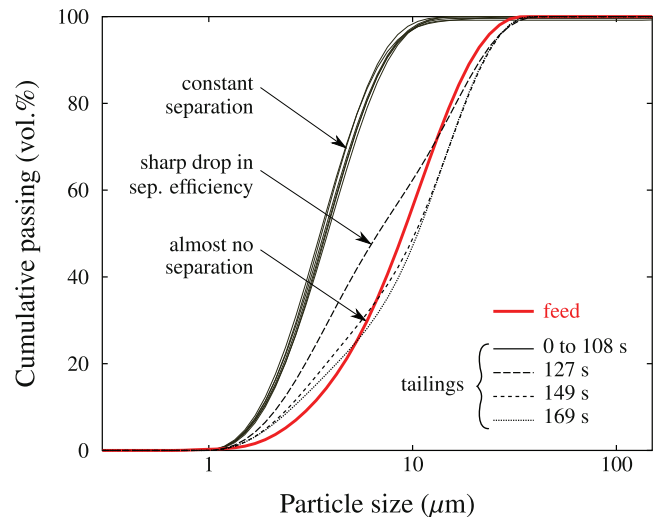


Fig. 4. Variation over time of size distribution in the tailings of Falcon L40 (operating conditions on Fig. 3).

gible [8]. This hypothesis implies that it is not necessary to account for particulate transport phenomena inside the bed in order to study and model the separation inside a Falcon concentrator. As this is a pivotal modeling hypothesis, we proceeded with experimental proof of this hypothesis. The procedure consisted in taking overflow samples over 3 min, and analyzing the size distribution of the samples. A typical result is plotted in Figs. 3 and 4 for operation of the concentrator at 4.45 L/min and 1460 rpm with a 0.5 mass% silica slurry. Fig. 3 shows the variation in mass flowrate as measured by the digital scale, where every sharp drop corresponds to the moment at which an overflow sample is being collected. For less than 2 min in this particular example, the size distribution of the overflow is unchanged, confirming that the separation inside the Falcon is stationary. Past this time, the separation efficiency drops sharply as indicated by the rapid change in the size distribution of the overflow, which then tends towards the feed size distribution. The transition between both regimes (which occurs between the samples taken at 108 and 127 s in the example) corresponds to the moment at which the retention zone is full. Laplanche et al. [5,13] have already described this situation, stating that particles can then no longer enter the retention zone unless they are fine enough to find a path inside the voids of the bed, or heavy enough to expel lighter particles outside the bed. The observation

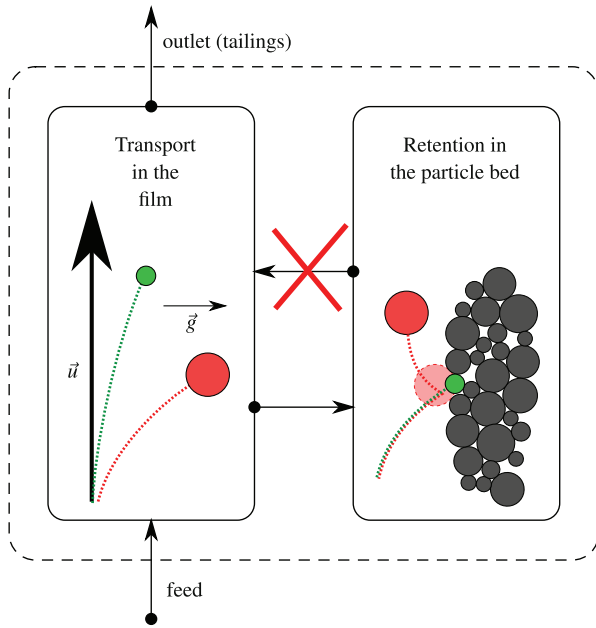


Fig. 5. Schematic illustration of model hypotheses, emphasizing no-resuspension.

that the particle size distribution towards which the overflow converges is somewhat finer than the feed size distribution would seem to indicate that heavier particles tend to enter the particle bed and expel finer particles back into the overflow.

Notwithstanding, the experimental data prove that the UF Falcon concentrator operates at steady-state until such a time as the retention zone is full. As shown on Fig. 5, if no resuspension from the retention zone happens, then differential settling rules separation. This mechanism being continuous, separation remains the same until retention zone is full and resuspension starts. In practice, this implies that provided the test is stopped before the retention zone is filled, the particles retained inside the bowl yield the size distribution of the concentrate stream.

3.2. Validation of the physics of the model by experimental calibration

The analytical model (1a) is based on a number of hypotheses about the physics of fluid and particle transport [8]. Moreover, it relies on certain parameters that are difficult to define precisely. Bowl length for example, noted as L_{bowl} in the model equation, is the length of a simplified bowl geometry with no cylindrical part (see Fig. 1). Since we have shown that the retention zone does play a negligible role in the separation, we neglect the true geometry of the bowl. Hence, the length that enters Eqs. (1a) and (2) is not precisely the real bowl length. The same applies to the opening angle (β) of the bowl. The actual rotation rate (ω) to be used in the model may not be exactly that of the bowl as the impeller may not transmit all its rotation speed to the suspension at the bottom of the bowl. As a result, one single calibration factor (λ) that bundles together the above issues must be added into the partition function expressions given in (1a) and (2), so that these expressions can have a true predictive value. The calibration constant is only here to account for quantitative correction for the physical counterparts of the model's theoretical parameters, but it should not hide any physics. That is why only one calibration constant is used, so predicted scaling according to different operating parameters can be compared between experiments and predictions. The value of this constant ($\lambda = 0.68$) being in the order of magnitude of 1, it also warrants that it only acts as correction but does not question the model validity. The fact of the matter is that should a single

calibration constant be sufficient for fitting our model to all the experimental data, then the assumptions we made about the physics of the process, which led to analytical expression (1a) would be validated. This is precisely what is verified hereafter.

The fraction (C) of each particle size and density class (r_p, ρ_p) that reports to the concentrate can be predicted by combining the model partition function (C_p) with the feed washability (f_{feed}), according to (3):

$$C = \iint f_{\text{feed}}(r_p, \rho_p) C_p(r_p, \rho_p) dr_p d\rho_p. \quad (3)$$

Since our UF Falcon model is phenomenological, it captures the physics of fluid and particle transport. Consequently, experimental testing of the model can be done using one type of particle only, such that feed washability is equal to the particle size distribution (one single density). This simple means of measuring washability makes the comparison between experimental and model predictions straightforward.

3.2.1. Recovery to tailings

With the silica particles described in Section 2.2, several experiments were carried out for different values of flowrate and rotation rate in the range 1–5 L/min and 1000–2500 rpm, respectively. Fig. 6 shows the experimental values of solids recovery to overflow, the circles showing the experimental error. The recovery of solids to the tailings (overflow) stream was predicted using (1a), with all parameters expressed in S.I. units, using the following values:

- flow (Q) and rotation (ω) rates as set in the experiments;
- density of the carrying fluid set to $\rho_f = 1.0 \text{ g/cm}^3$ (water);
- carrying fluid dynamic viscosity set to $1.0 \times 10^{-3} \text{ Pa s}$ (water);
- density of silica particles as measured by helium pycnometry, $\rho_p = 2.52 \text{ g/cm}^3$;
- particle size measured by laser sizing;
- bowl geometry: base radius $R_0 = 0.04 \text{ m}$, length $L_{\text{bowl}} = 0.07 \text{ m}$, opening angle $\beta = 20^\circ$ which gives $\alpha = 0.47$.

A least-squares regression was used to estimate the value of the constant λ from all the combined measurements from Fig. 6. The response surface of the model, which is shown in Fig. 6, yielded a remarkably good agreement between model predictions and measurements with a single value of the constant $\lambda = 0.68$. Confirmation of the goodness of fit of the model is given by the parity

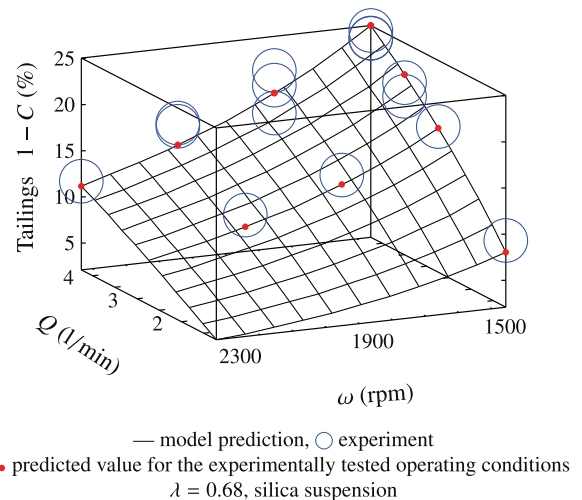


Fig. 6. Fitting of the model calibration factor against experimental data.

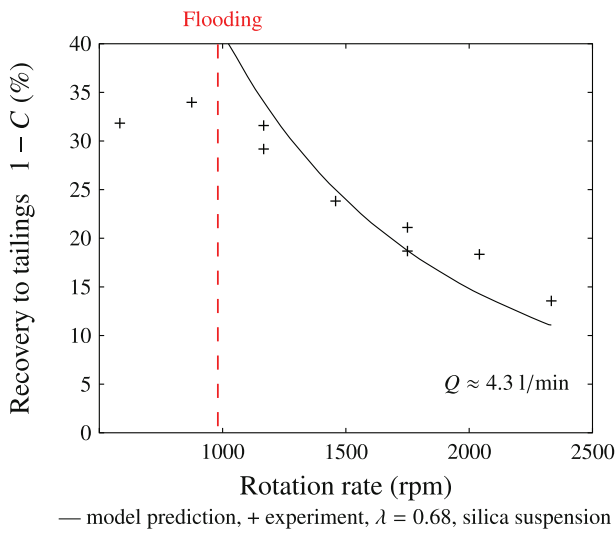


Fig. 7. Comparison of theoretical prediction and experimental evolution of separation with rotation rate.

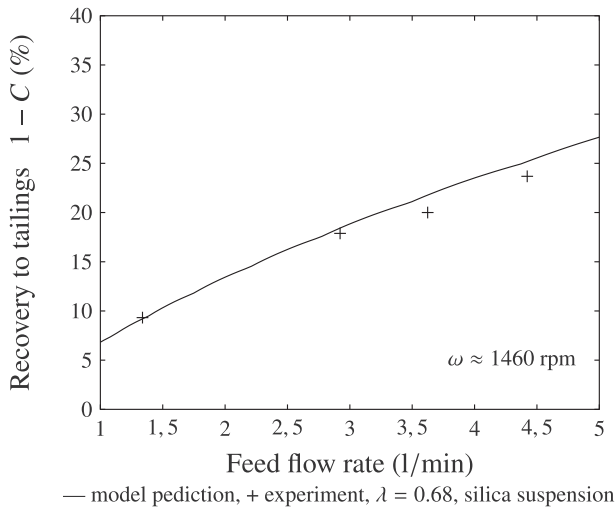


Fig. 8. Comparison of theoretical prediction and experimental evolution of separation with flow rate.

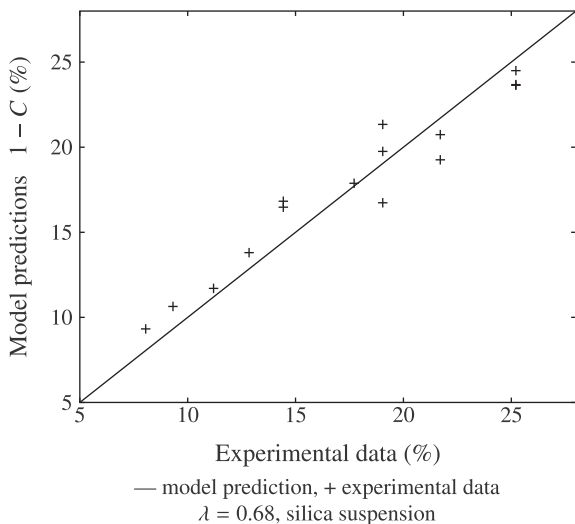


Fig. 9. Comparison between predicted recovery to tailings and experimental data.

diagram shown in Fig. 9, as well as the projections of the model response surface on the rotation rate and feed flowrate axes in Figs. 7 and 8, respectively. As discussed before, this result confirms the

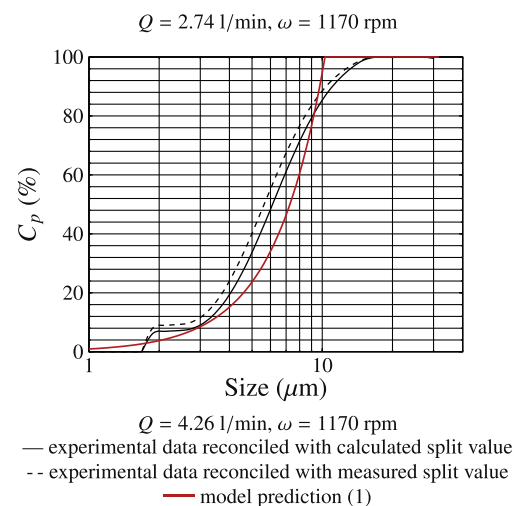
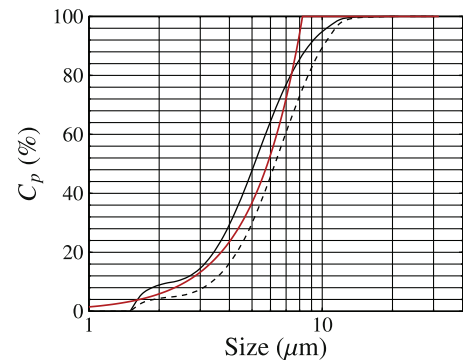
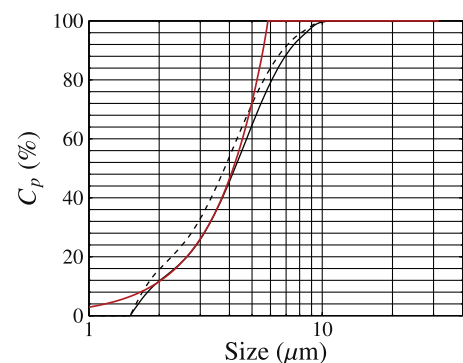
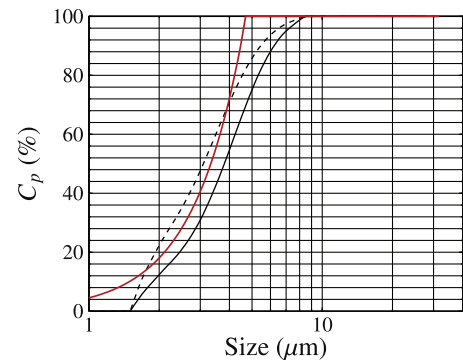


Fig. 10. Experimental partition functions and model prediction for silica suspension.

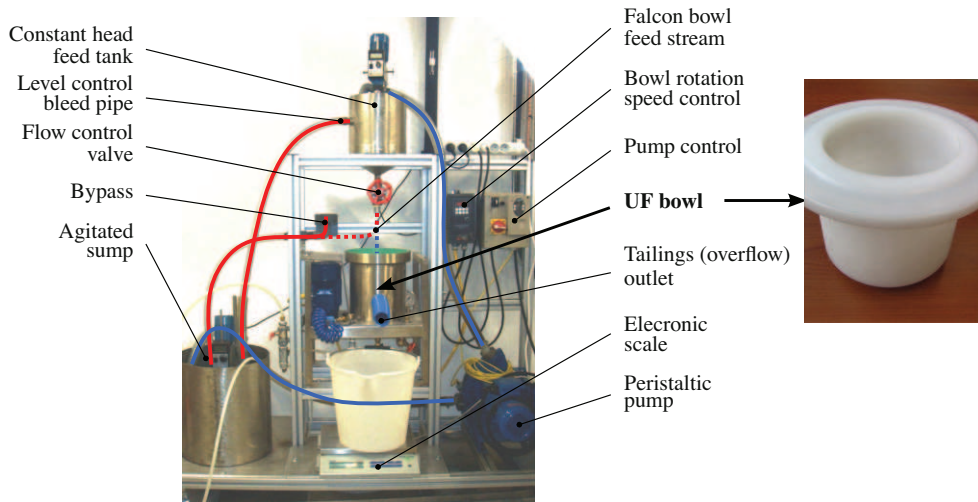


Fig. 11. Experimental setup of the Falcon concentrator L40.

physical hypotheses used to derive the proposed UF Falcon model. Moreover, the fact that the calibration constant is close to unity is another confirmation of the soundness of the proposed model.

Overall, the results obtained during this work reveal that the macroscopic behavior of the UF Falcon concentrator derives directly from the fundamental physical mechanisms that govern the separator. This is a remarkable result in itself, as it indicates that the performance of the separator is not hindered by design issues. This is a strong argument in favor of the robustness of this separator.

3.2.2. Partition function

The partition function [14] is estimated from the washability of all three streams. As we used single material slurries only for model validation, we recall that the washability we used is in fact the particle size distribution.

With balanced size distributions, solids split could be calculated from any measured size class.

$$\forall p, \quad C = \frac{[f_{\text{feed}}]_p - [f_{\text{tail}}]_p}{[f_{\text{conc}}]_p - [f_{\text{tail}}]_p}. \quad (4)$$

As with any such process, measured particle size distributions must be reconciled as they carry a certain amount of experimental error. In this work, a standard least-squares mass balancing technique using Lagrange multipliers was applied to the measured size distributions, using the most probable value of solids split, as described in [15]. The variance of the measurements, measured by repeating experimental tests, was used in the mass balancing calculations. In order to check the quality of the measured size distributions, reconciliation was also carried out directly with the measured solids split (measured from sampling both the feed and overflow streams). The closeness of the results obtained with data reconciled with both techniques is a direct confirmation of the quality of the measured size distribution.

Fig. 10 shows a number of measured versus predicted partition functions. The solid and dashed lines that are calculated with the measurements correspond to calculations with the two modes of reconciliation discussed earlier. They are given as confirmation of the quality of the measurements.

Overall, it is found that model predictions of partition functions are consistently in good agreement with the measured values. As calculations are all carried out with the earlier determined calibration constant $\lambda = 0.68$, these results are yet another confirmation of the soundness of the proposed model.

Partition functions are fundamental in that they fully characterize the separation efficiency of the UF Falcon separator. As Eq. (1a), which applies to dilute conditions only does not depend on feed washability, it can be used directly to predict the concentration of any given feed material. The extension of this model to concentrated suspensions (cf. Eq. (2)) is available in [9].

4. Conclusions and perspectives

In this paper, a phenomenological model of the UF Falcon concentrator applicable to dilute suspensions is validated through experiments. The model is derived directly from physics and is proposed as a simple analytical equation that predicts the partition function of the separator. Experimental measurements carried out with fine silica particles have yielded validation of all the key model hypotheses, which confirms the physics that is embedded into the proposed model. The model requires a single calibration constant that was determined by regression for the UF Falcon model and bowl geometry used in this study. The model can be used directly for making quantitative prediction of the UF Falcon performance.

The UF Falcon model whose physics has been validated here has already been extended to concentrated suspensions [9,10]. This extended model will be the object of an upcoming publication, which will also discuss the strengths and limitations of the UF Falcon concentrator for beneficiation of light and fine particles, such as with dredged sediments. Indeed, it is the environmentally significant question of beneficiation of dredged sediments that triggered this research about modeling and analysis of the separation performance of the UF Falcon concentrator. With our understanding of the physics of this concentrator, we are currently looking into applying this separator to a number of other areas of industrial significance, such as the beneficiation of coal fines, which has already been receiving attention [16–19] in the literature.

Acknowledgments

This work was funded by the French “Agence Nationale pour la Recherche” (ANR), in the framework of the PRECODD-PROSPED project. The authors also thank the Sibelco company for supplying silica samples and Mrs. Christine Rey-Rouch from the Laboratoire de Génie Chimique for her help on size distribution measurements.

References

- [1] R.L. Abela, Centrifugal concentrators in gold recovery and coal processing, in: *Extraction Metallurgy Africa*.
- [2] A. Chatterjee, Role of particle size in mineral processing at Tata Steel, *International Journal of Mineral Processing* 53 (1998) 1–14.
- [3] A.K. Majumder, J.P. Barnwal, Modeling of enhanced gravity concentrators – present status, *Mineral Processing & Extractive Metallurgy Review* 27 (2006) 61–86.
- [4] S.A. McAlister, K.C. Armstrong, Development of the Falcon concentrator, in: *Society for Mining, Metallurgy and Exploration Annual Meeting*.
- [5] A.R. Laplante, M. Buonvino, A. Veltmeyer, J. Robitaille, G. Naud, A study of the Falcon concentrator, *Canadian Metallurgical Quarterly* 33 (1994) 279–288.
- [6] C. Deveau, S.R. Young, Pushing the limits of gravity separation, in: *Society for Mining, Metallurgy and Exploration Annual Meeting*.
- [7] C. Deveau, Improving fine particle gravity recovery through equipment behavior modification, in: *38th Annual Meeting of the Canadian Mineral Processors*, Paper 31, pp. 501–517.
- [8] J.-S. Kroll-Rabotin, F. Bourgeois, E. Climent, Fluid dynamics based modelling of the Falcon concentrator for ultrafine particle beneficiation, *Minerals Engineering* 23 (2010) 313–320 (Special Issue: Physical Separation).
- [9] J.-S. Kroll-Rabotin, Analyse physique et modélisation de la séparation centrifuge de particules ultrafines en film fluant: application au séparateur industriel Falcon, Ph.D. Thesis, Institut National Polytechnique de Toulouse, 2010.
- [10] J.-S. Kroll-Rabotin, F. Bourgeois, E. Climent, Beneficiation of concentrated ultrafine suspensions with a falcon uf concentrator, in: *43rd Annual Meeting of the Canadian Mineral Processors*.
- [11] P. Kippax, Measuring particle size using modern laser diffraction techniques, *Paint & Coatings Industry Magazine* (2005).
- [12] E.G. Kelly, D.J. Spottiswood, *Introduction to Mineral Processing*, John Wiley & Sons, 1982.
- [13] A.R. Laplante, N. Nickoletopoulos, Validation of a Falcon model with a synthetic ore, *Canadian Metallurgical Quarterly* 36 (1997) 7–13.
- [14] B.A. Wills, T.J. Napier-Munn, *Wills' mineral processing technology: an introduction to the practical aspects of ore treatment and mineral recovery*, seventh ed., Butterworth-Heinemann, Oxford, 2006.
- [15] A. Lynch, *Mineral Crushing and Grinding Circuits – Their Simulation, Optimisation, Design and Control*, Developments in Mineral Processing, Elsevier Scientific Publishing Company, 1977.
- [16] R.Q. Honaker, B.C. Paul, D. Wang, K. Ho., Enhanced gravity separation: an alternative to flotation, in: *Society for Mining, Metallurgy and Exploration Annual Meeting*, High Efficiency Coal Preparation: An International Symposium.
- [17] R.Q. Honaker, High capacity fine coal cleaning using an enhanced gravity concentrator, *Minerals Engineering* 11 (1998) 1191–1199.
- [18] R.Q. Honaker, N. Singh, B. Govindarajan, Application of dense-medium in an enhanced gravity separator for fine coal cleaning, *Minerals Engineering* 13 (2000) 415–427.
- [19] F. Oruç, S. Özgen, E. Sabah, An enhanced gravity method to recover ultra-fine coal from tailings: Falcon concentrator, *Fuel* 89 (2010) 2433–2437.